

*Supporting information*

**Perfluorinated dibenzoylmethane in Ln<sup>3+</sup> Complexes: Charge-Transfer Quenching and Implications for Luminescence Design**

Alisia V. Tsorieva <sup>a</sup>, Vladislav M. Korshunov <sup>a,b</sup>, Victoria E. Gontcharenko <sup>a,c</sup>, Mikhail T. Metlin <sup>b</sup>, Tatiana S. Stankevich <sup>a,d</sup>, Victor O. Kompanets <sup>e</sup>, Sergey V. Chekalin <sup>e</sup> and Ilya V. Taydakov <sup>a</sup>

<sup>a</sup> P.N. Lebedev Physical Institute of the Russian Academy of Sciences, 53 Leninskiy 1. Prospect, 119991 Moscow, Russia

<sup>b</sup> Bauman Moscow State Technical University, 5/1 2-ya Baumanskaya Str., 105005 Moscow, Russia

<sup>c</sup> Faculty of Chemistry, National Research University Higher School of Economics, 20 Miasnitskaya Street, 101000 Moscow, Russia

<sup>d</sup> N. D. Zelinsky Institute of Organic Chemistry Russian Academy of Sciences, 47 Leninskiy Prospect, 119991 Moscow, Russia

<sup>e</sup> Institute of Spectroscopy of the Russian Academy of Sciences, 5 Fizicheskaya Ul., Moscow, 108840, Russia

\* Corresponding author. E-mail address: [taidakov@gmail.com](mailto:taidakov@gmail.com)

## SI-1. Crystal structures and powder X-ray diffraction (PXRD) data

**Table SI1.** Main crystallographic parameters and refinement details for **1Eu**, **1Gd** and **1Tb**

<i>Property</i>	<b>1Eu</b>	<b>1Gd</b>	<b>1Tb</b>
CCDC	2492487	2492489	2492488
Empirical formula	C <sub>57</sub> H <sub>11</sub> F <sub>30</sub> N <sub>2</sub> O <sub>6</sub> Eu	C <sub>57</sub> H <sub>11</sub> F <sub>30</sub> N <sub>2</sub> O <sub>6</sub> Gd	C <sub>57</sub> H <sub>11</sub> F <sub>30</sub> N <sub>2</sub> O <sub>6</sub> Tb
Formula weight (g·mol <sup>-1</sup> )	1541.64	1546.93	1548.60
T (K)	100(2)	100(2)	100(2)
Crystal system	triclinic	triclinic	triclinic
Space group	P -1	P -1	P -1
a (Å)	11.9675(4)	11.9449(3)	11.9117(3)
b (Å)	13.2543(4)	13.2468(3)	13.2793(4)
c (Å)	17.6498(5)	17.6143(5)	17.5854(4)
α (deg)	82.5870(10)	82.6380(10)	82.5660(10)
β (deg)	71.3540(10)	71.4250(10)	71.5970(10)
γ (deg)	85.1860(10)	85.2550(10)	85.1880(10)
V (Å <sup>3</sup> )	2627.79(14)	2617.57(12)	2614.46(12)
Z	2	2	2
D <sub>calc</sub> (g·cm <sup>-3</sup> )	1.948	1.963	1.967
θ <sub>min</sub> -θ <sub>max</sub> (deg)	1.798 - 30.505	1.552 - 30.548	1.548 - 29.000
μ (mm <sup>-1</sup> )	1.358	1.432	1.518
T <sub>min</sub> /T <sub>max</sub>	0.5816/0.6478	0.5508/0.6478	0.5625/0.6478
Reflections/Unique	29540/15863	29683/15890	26529/13790
Reflections with I>2σ(I)	14369	13252	11418
R <sub>int</sub>	0.0263	0.0425	0.0453
Goof	1.012	1.030	1.010
R <sub>1</sub> , wR <sub>2</sub> (I > 2σ(I))	0.0264, 0.0555	0.0409, 0.0802	0.0393, 0.0780
R <sub>1</sub> , wR <sub>2</sub> (all data)	0.0315, 0.0572	0.0545, 0.0847	0.0538, 0.0828

**Table SI2.** Shape analysis of Ln<sup>3+</sup> coordination polyhedra in **1Eu**, **1Gd**, **1Tb**

Compound	Cube (O <sub>h</sub> )	Square antiprism (D <sub>4d</sub> )	Triangular dodecahedron (D <sub>2d</sub> )	Biaugmented trigonal prism (C <sub>2v</sub> )	Triakis tetrahedron (T <sub>d</sub> )
<b>1Eu</b>	10.143	<b>1.271</b>	1.081	2.074	10.802
<b>1Gd</b>	10.128	<b>1.274</b>	1.088	2.079	10.782
<b>1Tb</b>	10.180	<b>1.213</b>	1.095	2.017	10.836

**Table SI3.** Ln-O bond lengths in corresponding complexes.

Ln-O bond length, Å	<b>1Eu</b>	<b>1Gd</b>	<b>1Tb</b>
Ln-O1	2.3329(12)	2.3303(19)	2.315(4)
Ln-O2	2.3837(12)	2.3782(18)	2.359(2)
Ln-O3	2.3076(12)	2.3072(19)	2.287(2)

Ln-O4	2.3820(12)	2.3803(18)	2.371(2)
Ln-O5	2.3601(12)	2.3538(19)	2.338(2)
Ln-O6	2.3998(12)	2.3949(18)	2.388(2)
Ln-N1	2.5389(14)	2.532(2)	2.526(2)
Ln-N2	2.6127(14)	2.611(2)	2.595(2)
Mean Ln-O	2.36	2.35	2.34
Mean Ln-N	2.58	2.57	2.56

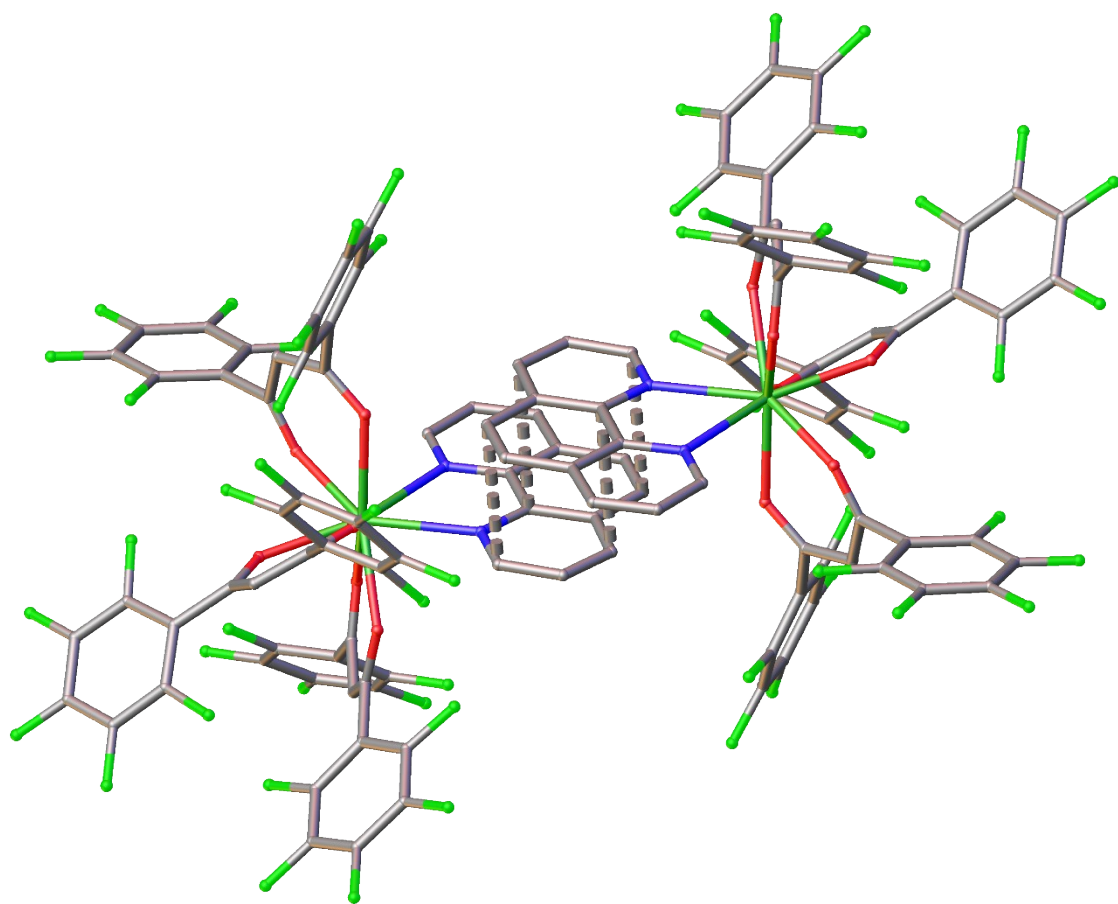


**Figure S11.**  $\pi$ -stacking (shown in dashed lines) between 1,10-phenanthroline moieties in **1Gd**. Thermal ellipsoids of atomic displacement, as well as hydrogen atoms, are omitted for clarity. The second molecule corresponds to symmetry code  $(1-x, 2-y, -z)$ .

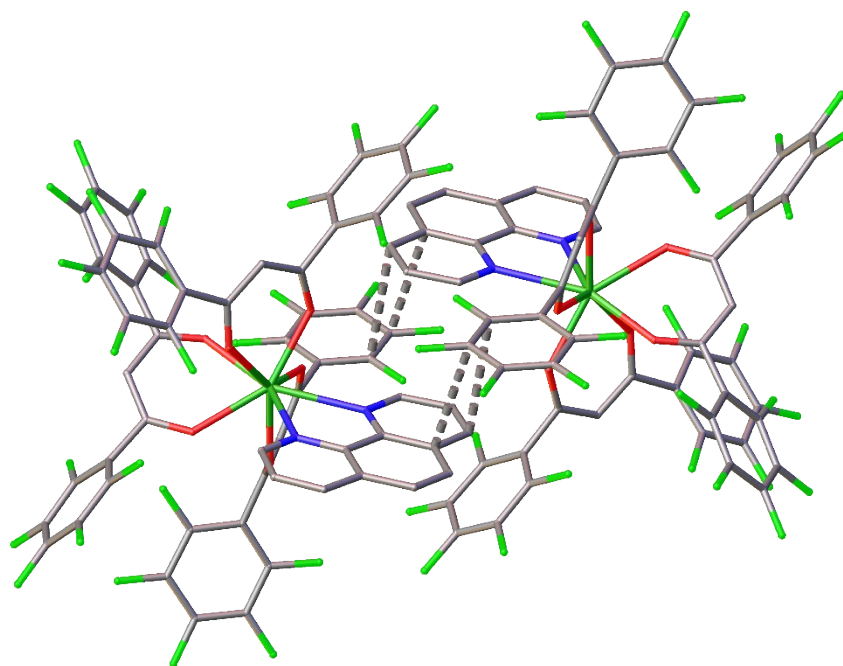


**Figure S12.**  $\pi$ -stacking (shown in dashed lines) between 1,10-phenanthroline and perfluorophenyl moieties in **1Gd**. Thermal ellipsoids of atomic displacement, as well as hydrogen atoms, are omitted for clarity. The second molecule corresponds to symmetry code ( $1-x, 1-y, -z$ ).

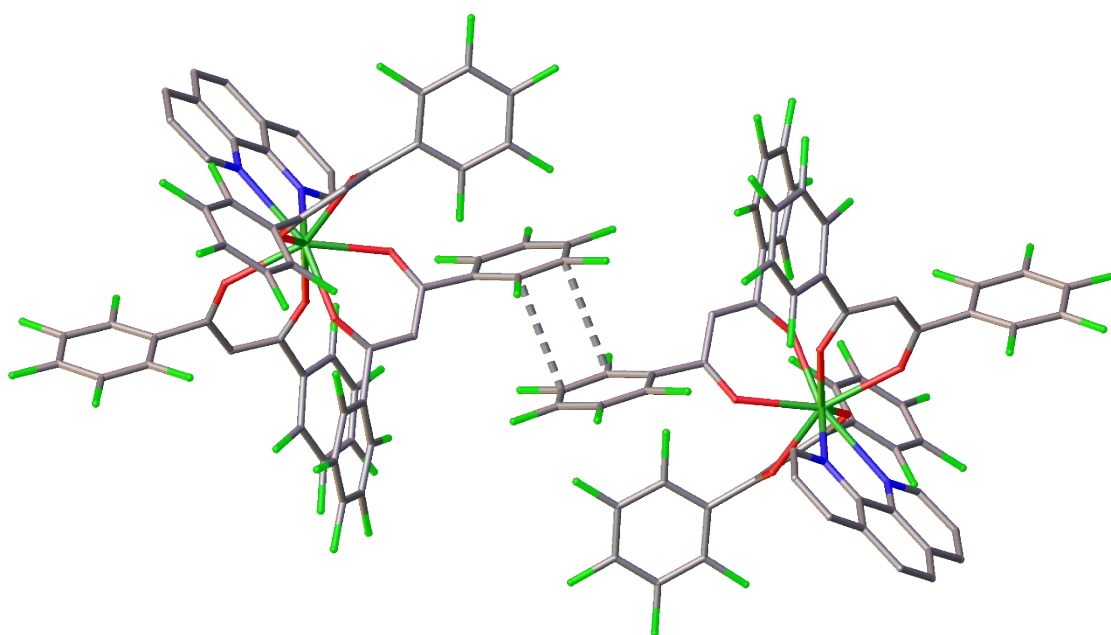


**Figure S13.**  $\pi$ -stacking (shown in dashed lines) between perfluorophenyl moieties in **1Gd**. Thermal ellipsoids of atomic displacement, as well as hydrogen atoms, are omitted for clarity. The second molecule corresponds to symmetry code ( $1-x, 2-y, 1-z$ ).

## SI-2. Photophysical studies

The UV-Vis spectra for MeCN dissolved **1Eu**, **1Tb** complexes and free ligand **HPFDBM** are shown in Figure S1. The absorption band located at ca. 350 nm is associated with electronic  $\pi$ - $\pi^*$

transitions of  $\beta$ -diketone fragment.<sup>1</sup> The peaks at 270 and 293 nm correspond to *1,10*-phenanthroline.

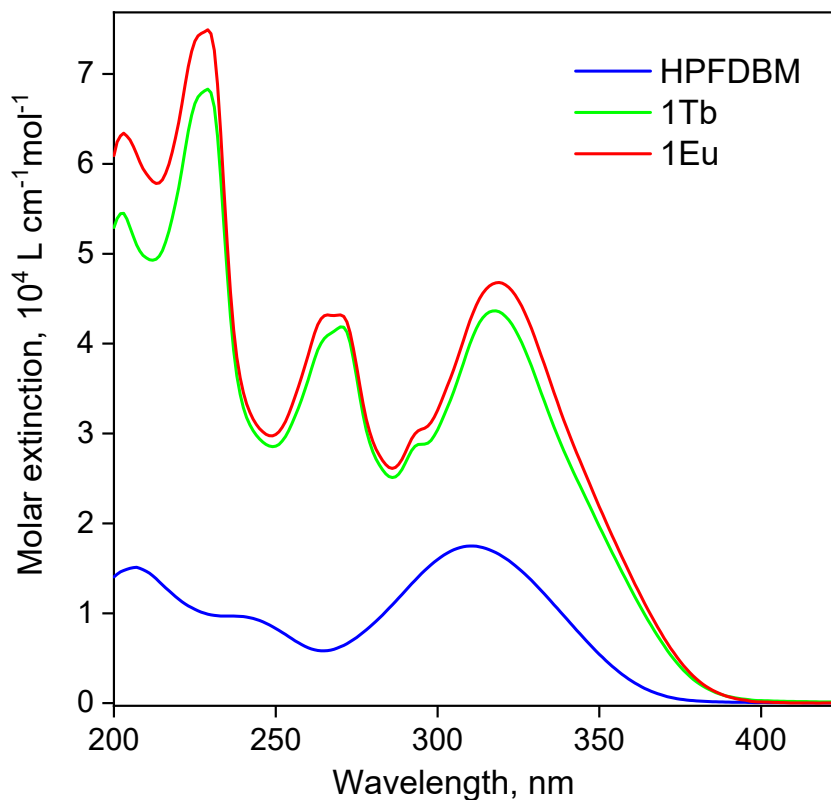


**Figure SI4.** UV-vis spectra for the investigated **1Tb** and **1Eu** complexes and free ligand dissolved in MeCN

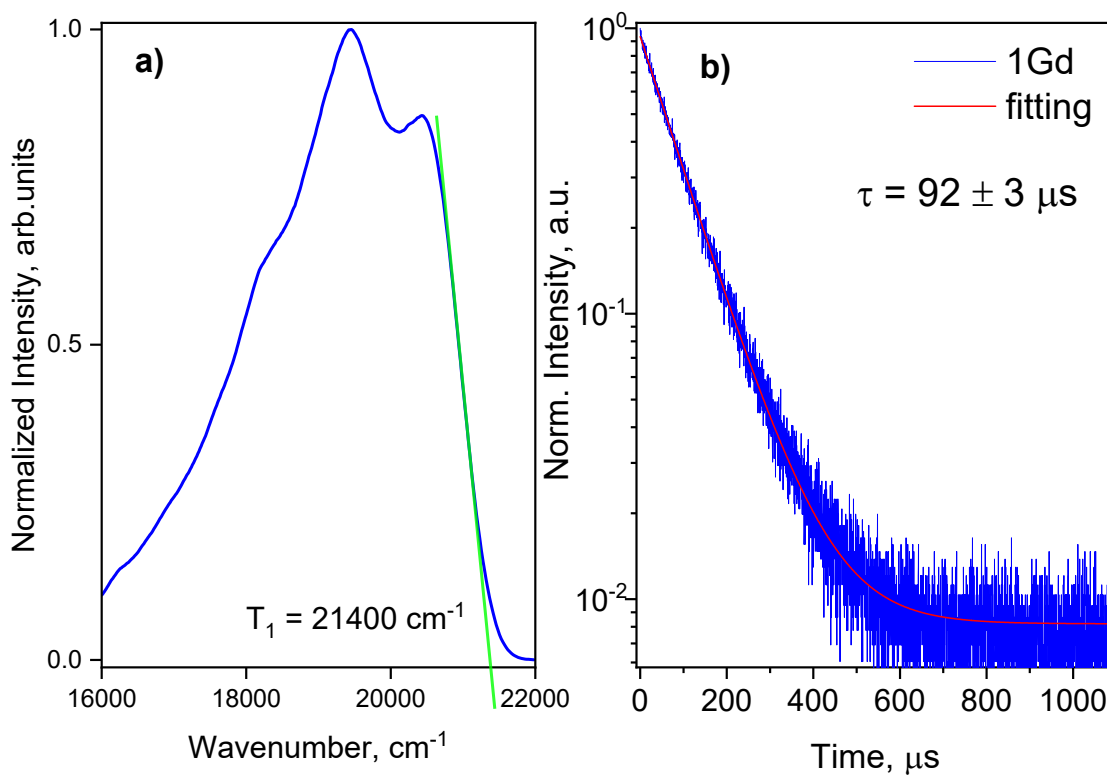


**Figure SI5. a)** The phosphorescence spectra for solid state **1Gd** compound normalized on the maximum intensity recorded upon excitation at 350 nm at 77 K with 10  $\mu$ s time delay; **b)** PL decay for **1Gd** measured upon excitation at 360 nm recorded at 520 nm at 300 K

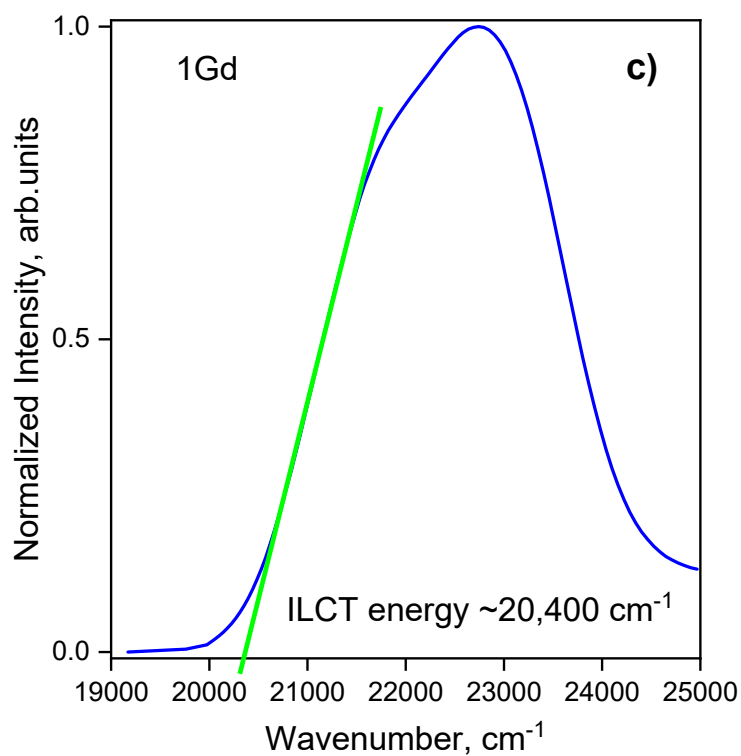


**Figure SI5. c)** Visualization of tangent method applied to the excitation spectrum of **1Gd** compound.

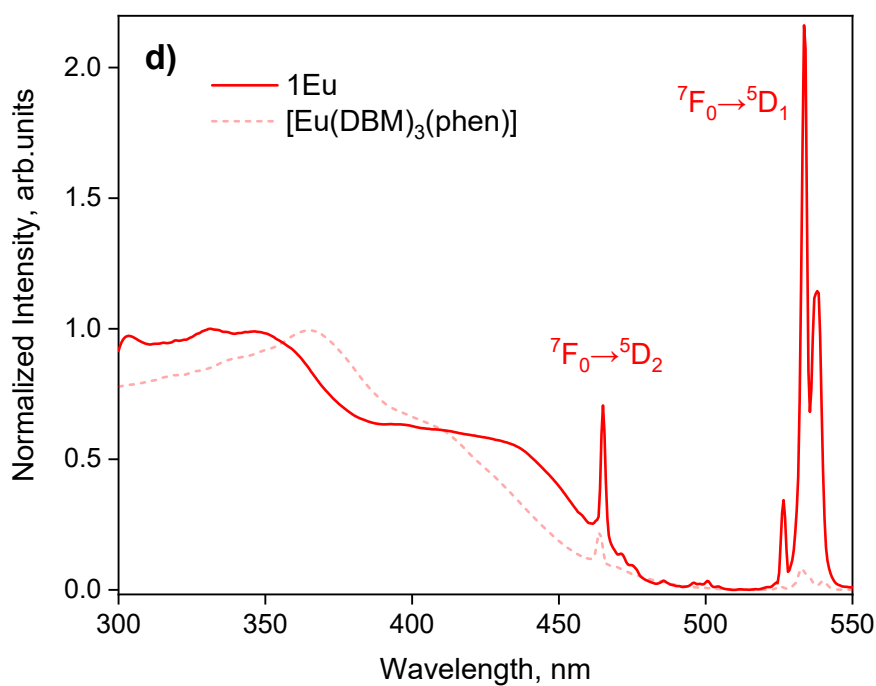


**Figure S15.** d) PL excitation spectra for crystalline powder complexes recorded at 615 nm for **1Eu** and **[Eu(DBM)<sub>3</sub>(phen)]** normalized on maximum PL ligand intensity

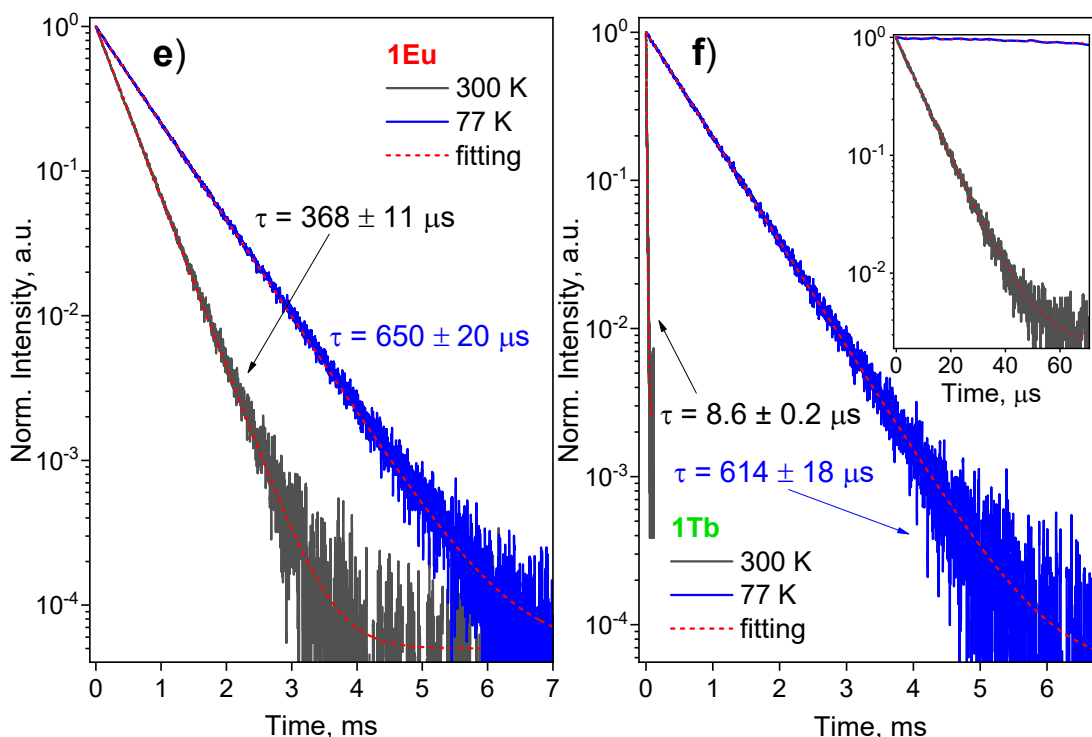


**Figure S15.** e) PL decay for **1Eu** measured upon excitation at 360 nm recorded at 615 nm at 300 K; f) PL decay for **1Tb** measured upon excitation at 360 nm recorded at 520 nm at 300 K. In the simplest case, the relaxation of excited states explained by a two-level model (relaxation of strictly one excited state). It obeys a monoexponential law

$$I(t) = I_0 e^{-\frac{t}{\tau_{obs}}},$$

where the lifetime  $\tau_{obs}$  observed in the experiment is defined as

$$\tau_{obs} = \frac{1}{k_{obs}} = \frac{1}{k_{rad} + k_{nrad}},$$

$k_{rad}$  and  $k_{nrad}$  – the rate constants of radiative and nonradiative relaxation, respectively.

The value of the internal quantum yield can be estimated by the following formula

$$\Phi_{Ln} = \frac{k_{rad}}{k_{rad} + k_{nrad}}.$$

Since the value of the rate constant of the magnetic-dipole transition  ${}^5D_0-{}^7F_1$  in  $\text{Eu}^{3+}$   $k_{MD}=14.65 \text{ s}^{-1}$  does not depend on the electric field induced by the ligand, it is possible to determine the value of  $k_{rad}$  by the relation

$$k_{rad} = k_{MD} n^3 \frac{I_{tot}}{I_{MD}},$$

where  $n$  – the refractive index,  $I_{tot}/I_{MD}$  – the ratio of the total integral luminescence intensity to the integral intensity of the magnetic-dipole transition. The constant  $k_{nrad}$  was evaluated using a simple dependency

$$k_{nrad} = \frac{1}{\tau_{obs}} - k_{rad},$$

including the calculated  $k_{rad}$  and the observed attenuation time  $\tau_{obs}$ , measured with resonant excitation of  $\text{Eu}^{3+}$  at the wavelength 532 nm. The calculated value of the internal PL quantum yield  $\Phi_{Ln}$ , the value of the total PL quantum yield  $\Phi$  measured by the absolute method, the sensitization coefficient  $\eta$  are presented in Table SI4.

**Table SI4.** Photophysical parameters for crystalline powder complexes:  $k_{rad}$  and  $k_{nrad}$  – radiative and non-radiative processes rates, the back energy transfer (BET) process rate ( $k_{BET}$ ), the internal quantum yield ( $\Phi_{Ln}$ ), the overall quantum yield ( $\Phi$ ) and the sensitization efficiency  $\eta$ .

Compound	$I_{tot}/I_{MD}$	$k_{rad}, \text{ s}^{-1}$	$k_{nrad}, \text{ s}^{-1}$	$k_{BET}, \text{ s}^{-1}$	$k_{vib}, \text{ s}^{-1}$	$\tau_{obs}^{-1}, \text{ s}^{-1}$	$\Phi_{Ln}, \%$	$\Phi, \%$	$\eta$
<b>[Eu(DBM)<sub>3</sub>(phen)]*</b>	25.5	1,262	1,288	407	881	2,550	49.5	23.3	0.47
<b>1Eu</b>	20.0	989	1,814	554	1,260	2,803	35.3	2.0	0.014

\* The results except  $k_{BET}$  and  $k_{vib}$  are obtained in the work<sup>2</sup>

The Arrhenius equation is given by

$$\ln\left(\frac{1}{\tau_{300}} - \frac{1}{\tau_T}\right) = \ln(k_{BET}) = \ln(A) - \frac{\Delta E_A}{R} T^{-1},$$

where  $\tau_{300}$ ,  $\tau_T$ ,  $R$  and  $T$  are an emission lifetime at 300 K, emission lifetime at  $T$  temperature, gas constant and compound temperature, respectively.<sup>3</sup>

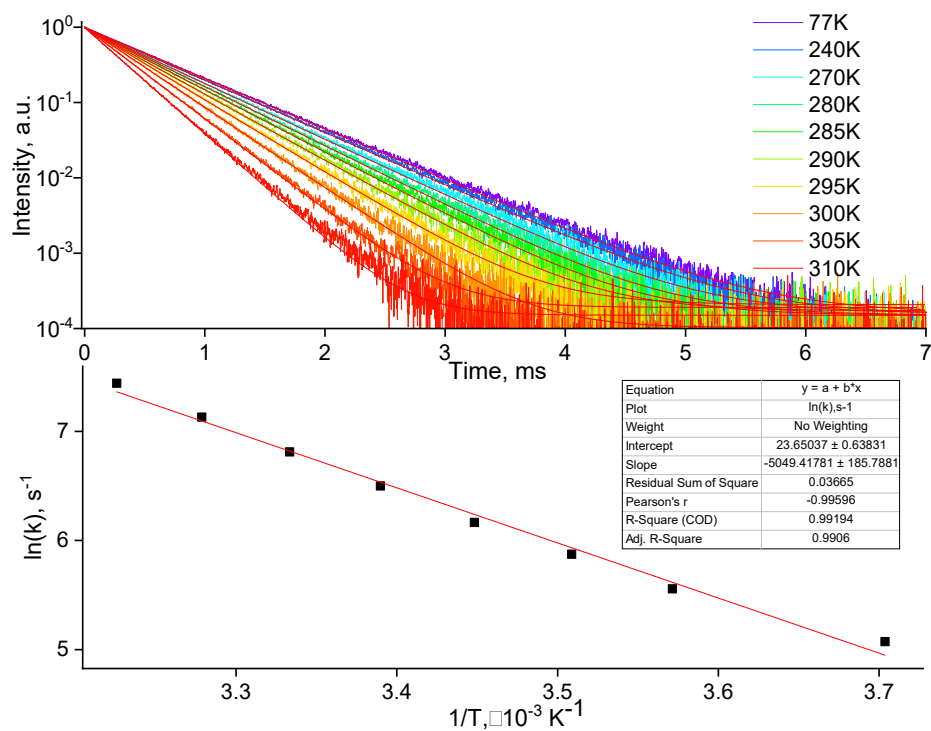


**Figure SI6.** Temperature-dependent emission decays for **1Eu** compound in solid state at temperatures of 78-300 K under pulsed excitation at 360 nm.

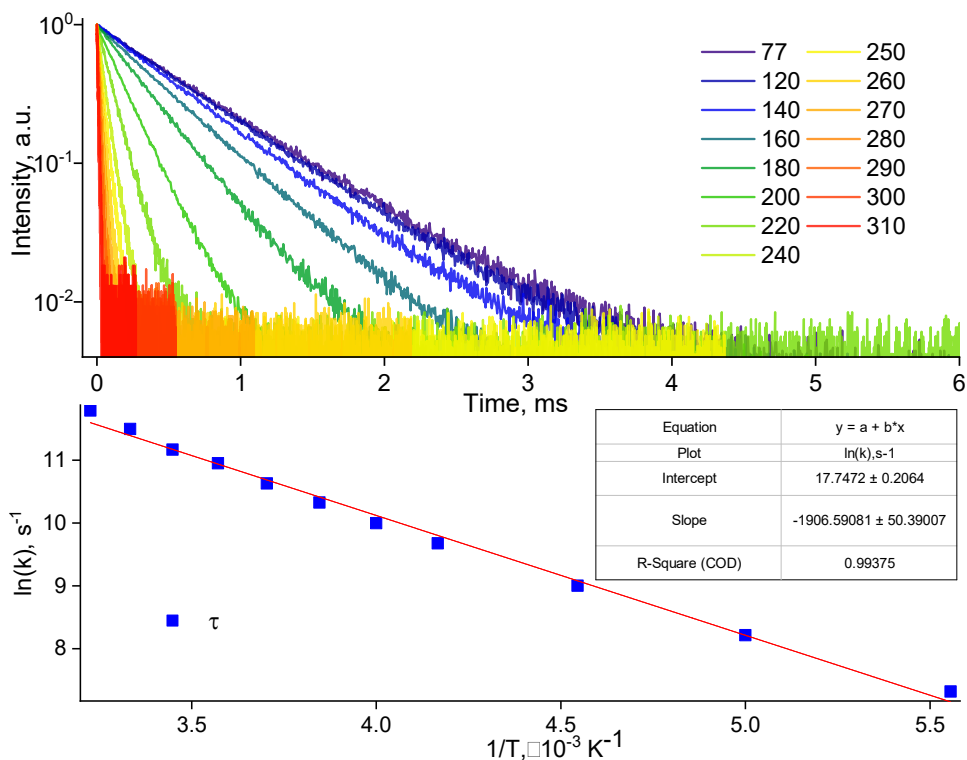


**Figure SI7.** Temperature-dependent emission decays for **1Tb** compound in solid state at temperatures of 78-300 K under pulsed excitation at 360 nm.

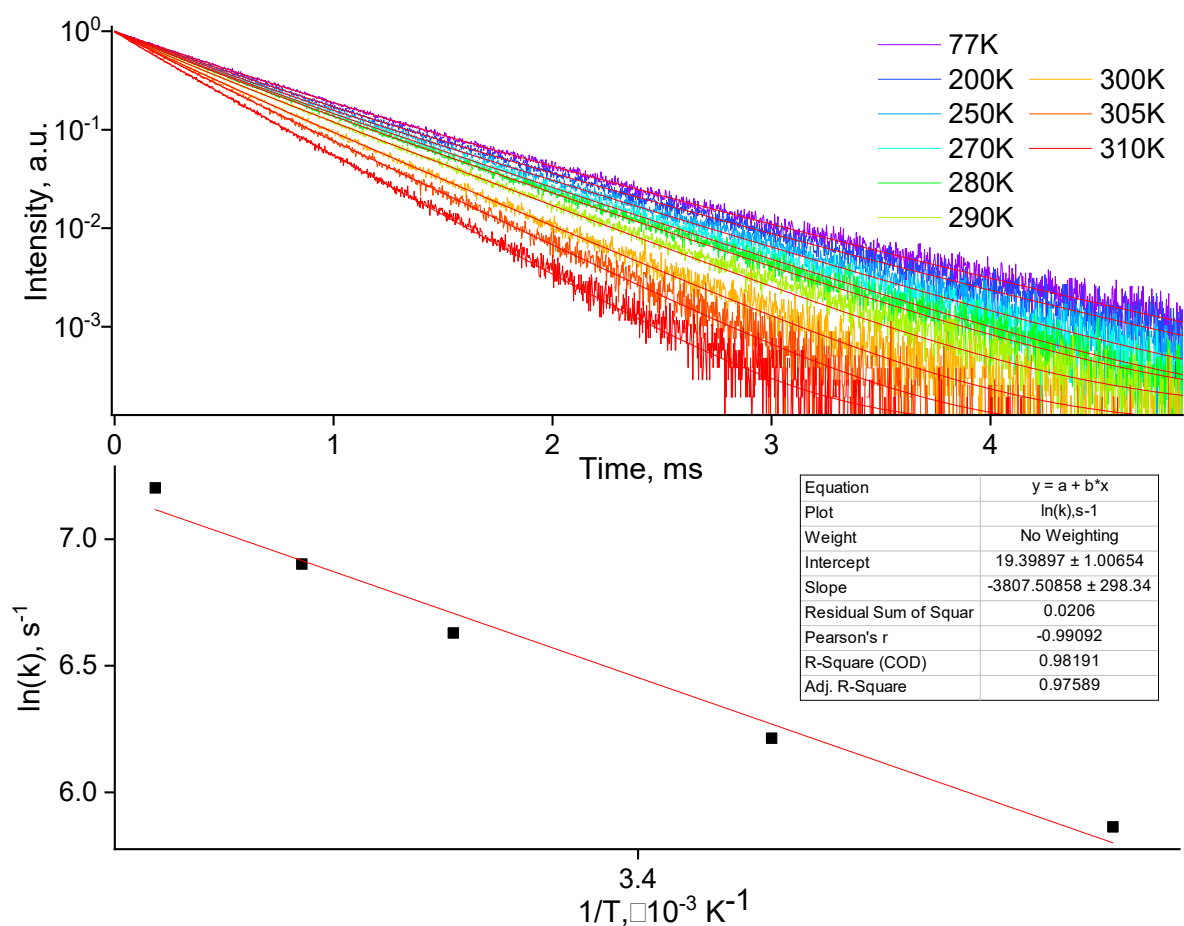


**Figure S18.** Temperature-dependent emission decays for **[Eu(DBM)<sub>3</sub>(phen)]** compound in solid state at temperatures of 78-300 K under pulsed excitation at 360 nm.

**Table S15.** The luminescence lifetimes ( $\tau$ ) estimated from temperature-dependent luminescence decays for the **[Eu(DBM)<sub>3</sub>(phen)]**, **1Eu** and **1Tb** compounds.

<b>[Eu(DBM)<sub>3</sub>(phen)]</b>		<b>1Eu</b>		<b>1Tb</b>	
T, K	$\tau$ , $\mu$ s	T, K	$\tau$ , $\mu$ s	T, K	$\tau$ , $\mu$ s
78	653	78	644	78	646
200	617	200	439	140	554
250	578	250	339	160	457
270	551	270	584	180	327.2
280	531	280	552	200	190.8
290	492	285	524	220	103.4
300	437	290	493	240	57.1
305	397	295	451	250	42.5
310	348	300	406.5	260	31.2
		305	357	270	23.3

		310	307	280	17,1
				290	13,8
				300	10
				310	7,5

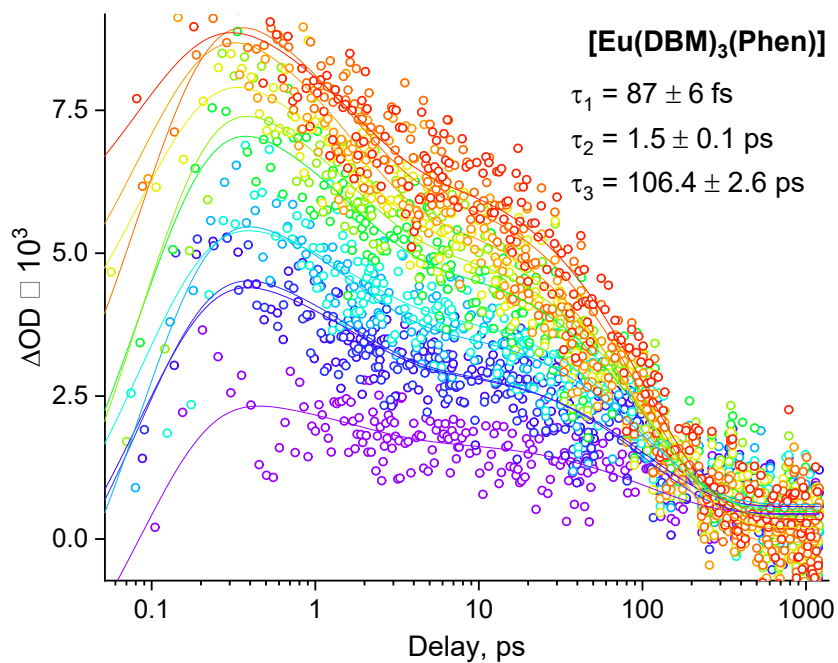


**Figure SI9.** Fs-TA kinetics for [Eu(DBM)<sub>3</sub>(phen)] at selected wavelengths.

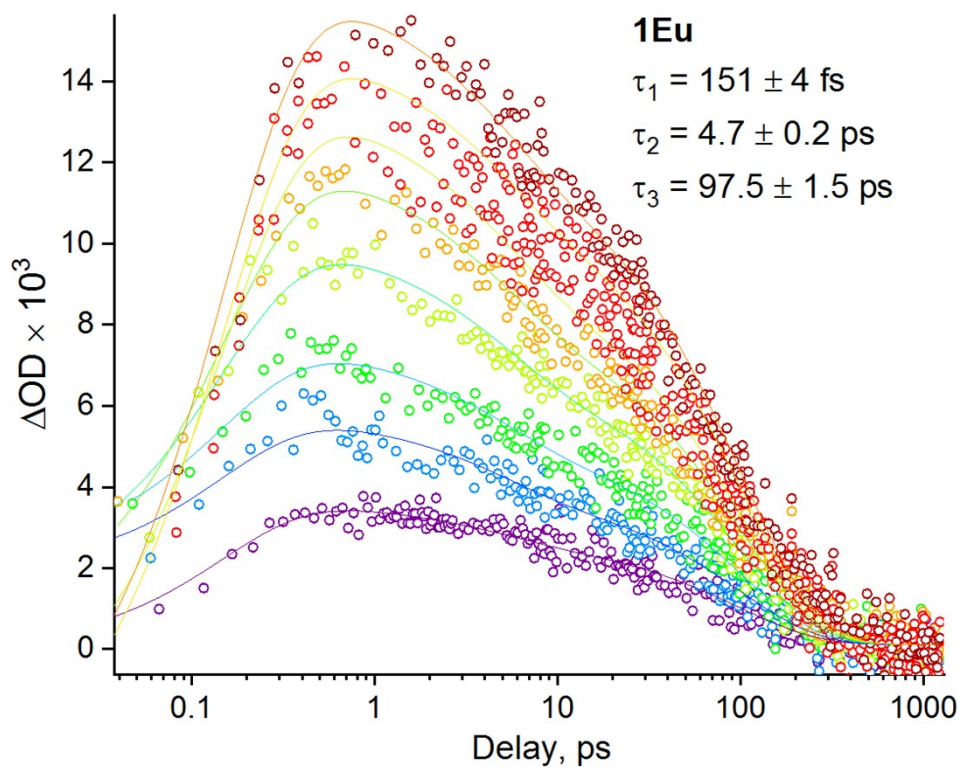


**Figure SI10.** Fs-TA kinetics for 1Eu at selected wavelengths.

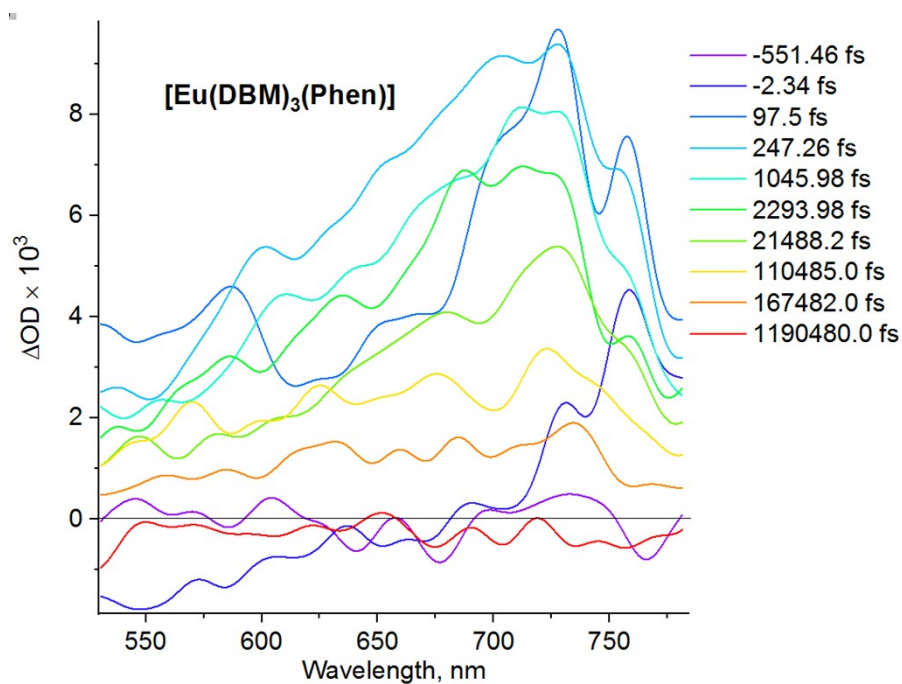


**Figure S111.** Fs-TA kinetics for  $[\text{Eu}(\text{DBM})_3(\text{phen})]$  for selected time delays.

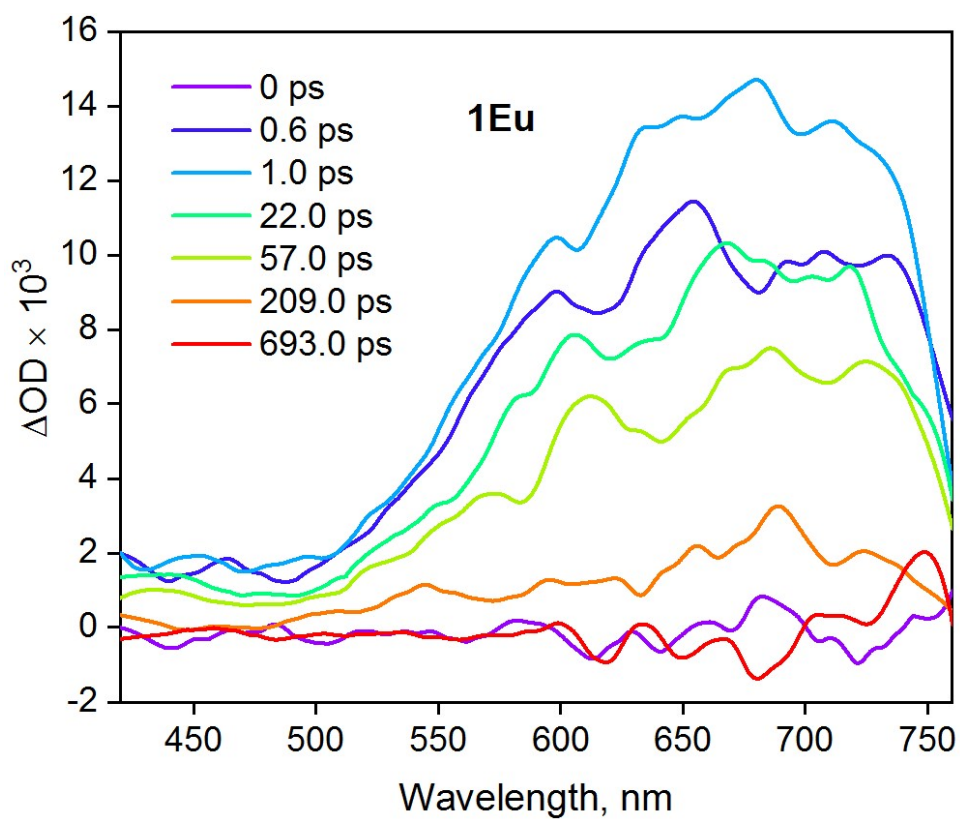


**Figure S112.** Fs-TA kinetics for  $1\text{Eu}$  for selected time delays.

### SI-3. Synthesis and characterization of ligand HPFDBM.

Column chromatography was performed on Silica gel 60 (50-200  $\mu\text{m}$  particle size) sorbents, both obtained from Macherey-Nagel.

$^1\text{H}$ ,  $^{19}\text{F}$  and  $^{13}\text{C}$  NMR spectra were obtained with a Bruker AM-300 or DRX-500 NMR spectrometer (at frequencies of 300.1/500.13, 282.4/470.1 and 75.5/125.76 MHz, respectively) in  $\text{CDCl}_3$  solutions, with TMS ( $^1\text{H}$ ,  $^{13}\text{C}$ ) or  $\text{CFCl}_3$  ( $^{19}\text{F}$ ) as a standards.  $J$  values are given in Hz. Multiplicities are assigned as s (singlet), d (doublet), t (triplet), q (quartet) and m (multiplet). High resolution mass spectra were measured on a Bruker micrOTOF II instrument using electrospray ionization (ESI). IR spectra were measured with a Bruker Alpha instrument in KBr pellets.

We were unable to obtain spectra of acceptable quality in  $\text{CD}_3\text{CN}$  or  $\text{CD}_3\text{OD}$  due to low solubility of complexes. Solubility in  $\text{CDCl}_3$  is incomparably higher; we were able to dissolve up to 25–30 mg of the complex in 1 mL, but it is evident that in this solvent the complexes are unstable and partially decompose. In our view, NMR spectra of complexes are of limited informative value; however, as one of the reviewers requested that they must be included in the paper, they have been added to the SI section.

#### **1,3-Bs(perfluorophenyl)propane-1,3-dione (HPFDBM).**<sup>4,5</sup>

Anhydrous  $\text{AlCl}_3$  (5.3 g, 40 mmol) was suspended in 30 mL of dry 1,1,2,2-tetrachloroethane and the 2,3,4,5,6-pentafluorobenzoyl chloride (5.8 mL, 9.2 g 40 mmol) is added dropwise within 10 min, while the mixture was protected from moisture by  $\text{CaCl}_2$  drying tube. The resulted solution was stirred for 1 h at a room temperature (22  $^\circ\text{C}$ ) and then vinyl acetate (3.8 mL, 3.45 g, 40 mmol) was added dropwise. Dark reaction mixture was stirred overnight at 30  $^\circ\text{C}$ , then carefully poured with stirring on mixture of ice (100 g) and 20 mL of conc. HCl. The solvent was evaporated, and residue separated by a column chromatography (silica,  $\text{C}_6\text{H}_6$ ). The diketone was obtained at  $R_f = 0.75$ , and two other byproducts were

obtained with  $R_f = 0.9$  ( $\text{Al}(\text{PFDBM})_3$ ) and 0.45 (1-(perfluorophenyl)butane-1,3-dione), respectively. The target compound was collected and recrystallized from 96% EtOH. Yield is 13 % (2.1 g). M. p. 82-83 °C (lit<sup>5</sup>. 83–84 °C).

$^1\text{H}$  NMR (300 MHz,  $\text{CDCl}_3$ , 100% enol form):  $\delta$  15.11 (s, OH), 6.25 (s, CH).

$^{13}\text{C}$  NMR (126 MHz,  $\text{CDCl}_3$ ):  $\delta$  176.4, 145.4 (d(m),  $J = 256$  Hz), 143.3 (d(m),  $J = 256$  Hz), 136.4 (d(m),  $J = 256$  Hz), 110.7 (m), 105.8 (s).

$^{19}\text{F}$  NMR (282MHz,  $\text{CDCl}_3$ ):  $\delta$  -135.6 – (-142.3) (m), -147.7 (tt,  $J = 20.9, 4.5$  Hz), -156.8 – (-164.4) (m).

IR (KBr pellet,  $\text{cm}^{-1}$ ): 3461, 3142, 2921, 1655 1590, 1519, 1489, 1330, 1322, 1212, 1183, 1100, 990, 936, 823, 648.

HRMS (EI)  $m/z$ :  $[\text{M}+1]^+$  Calcd for  $\text{C}_{15}\text{H}_2\text{F}_{10}\text{O}_2 + \text{H}$ : 404.9968; Found: 404.9963

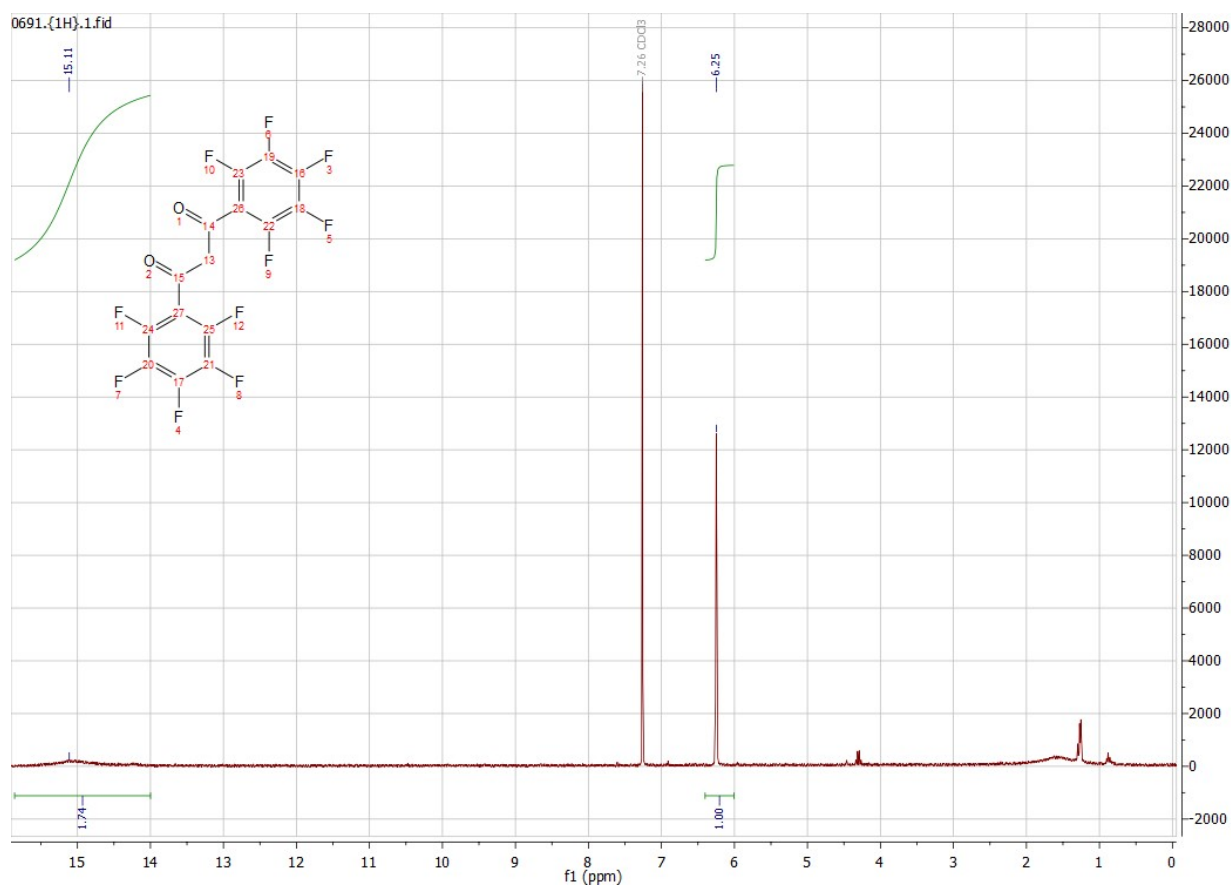


**Figure SI13.**  $^1\text{H}$ -NMR spectrum for HPFDBM in  $\text{CDCl}_3$

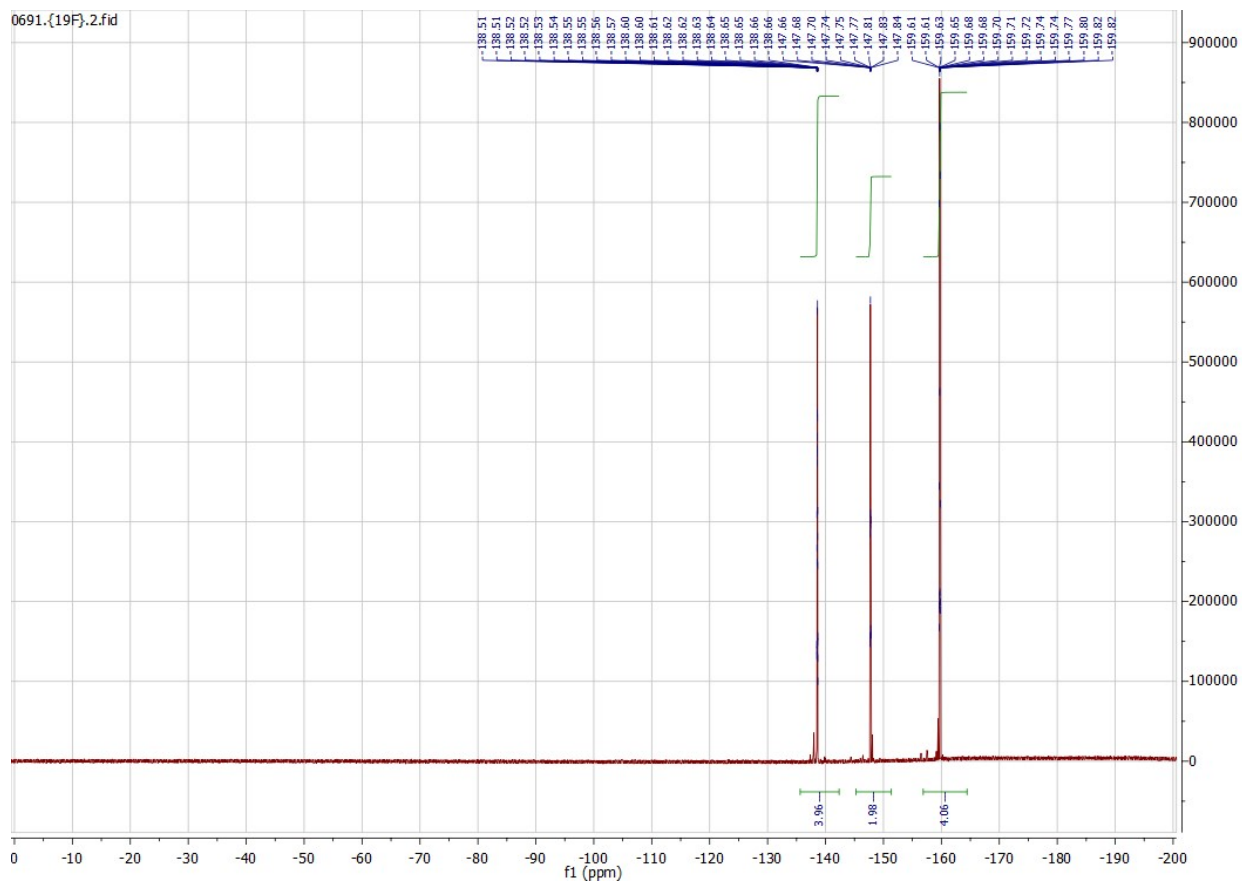


Figure S114.  $^{19}\text{F}$ -NMR spectrum for HPFDBM in  $\text{CDCl}_3$

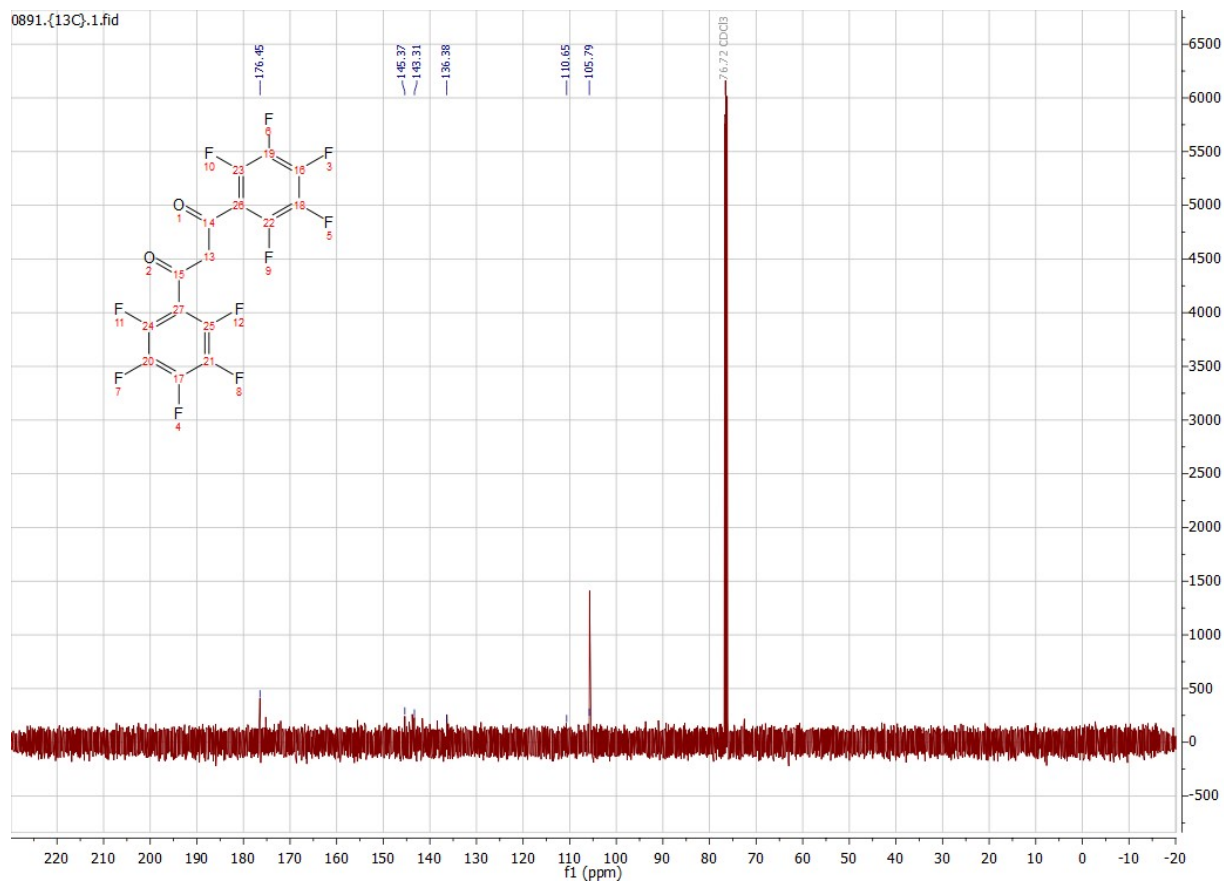


Figure S115.  $^{13}\text{C}$ -NMR spectrum for HPFDBM in  $\text{CDCl}_3$

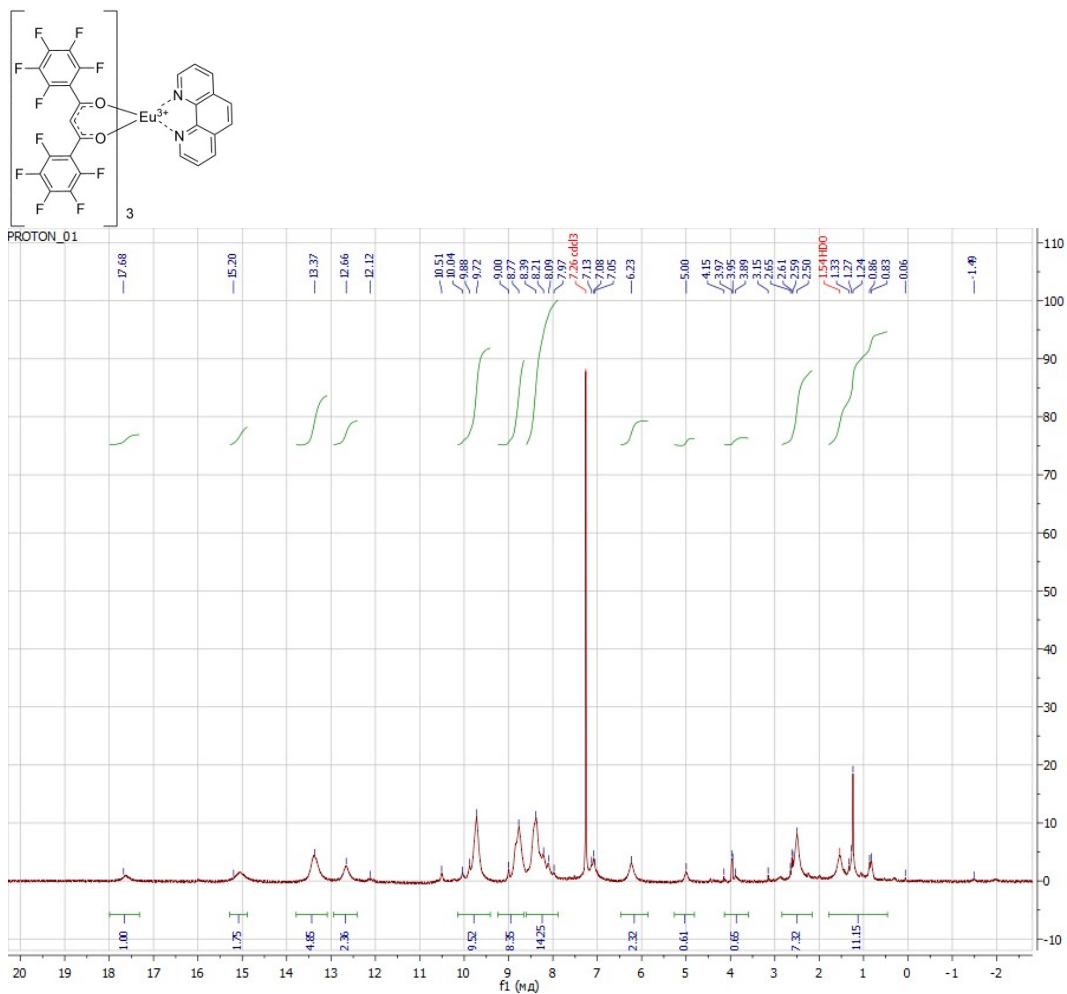


Figure SI16.  $^1H$ -NMR spectrum of  $[Eu(PFDMB)_3Phen]$  in  $CDCl_3$

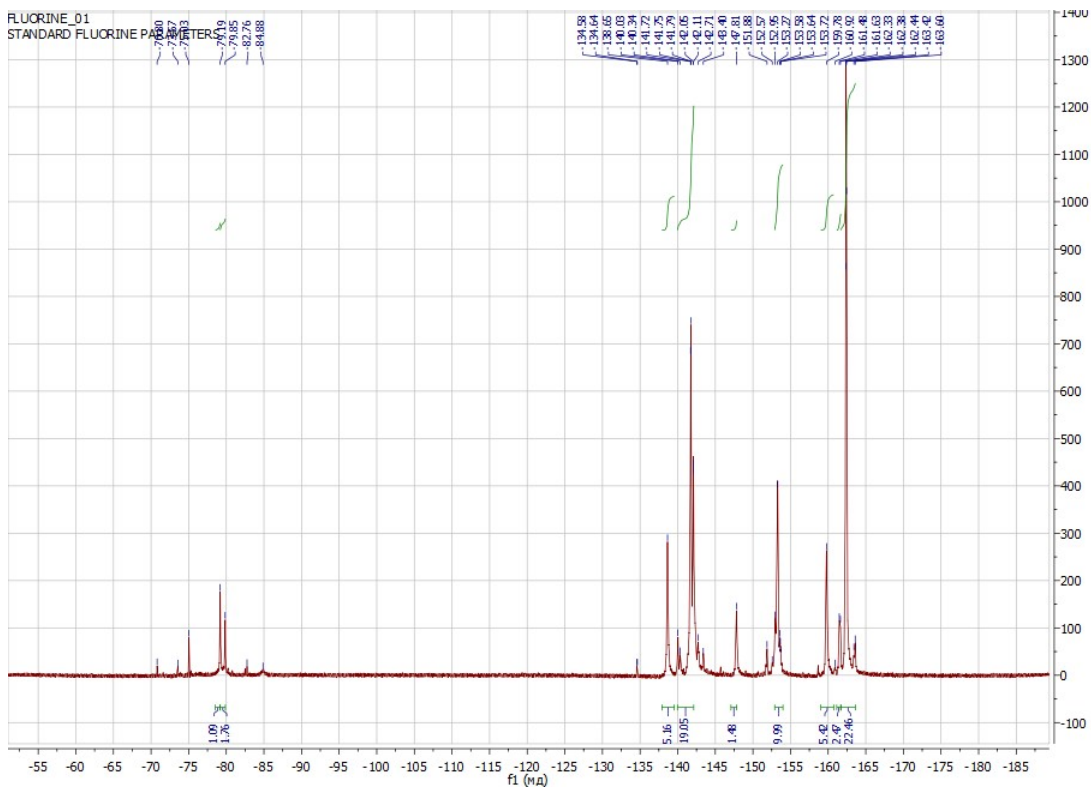


Figure SI17.  $^{19}F$ -NMR spectrum of  $[Eu(PFDMB)_3Phen]$  in  $CDCl_3$

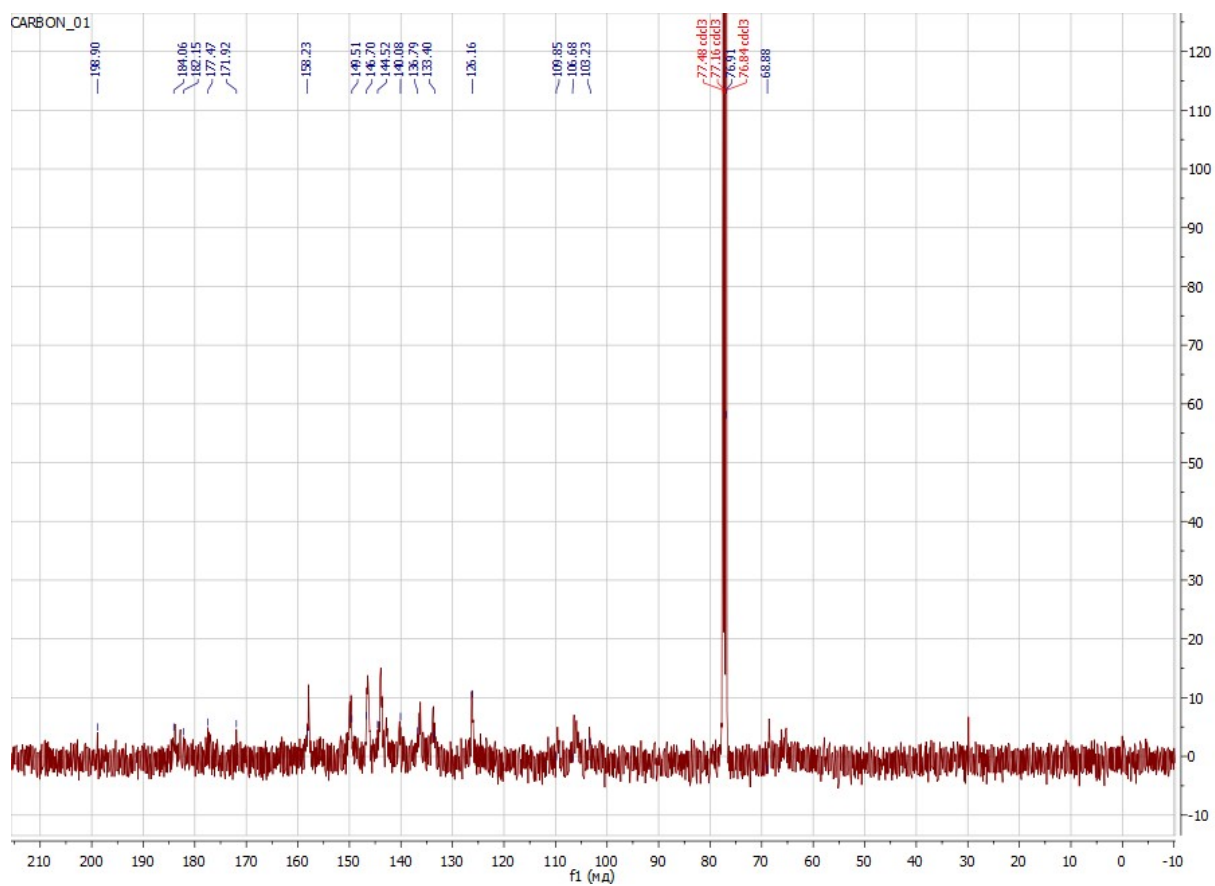


Figure S118.  $^{13}\text{C}$ - NMR spectrum of  $[\text{Eu}(\text{PFDMB})_3\text{Phen}]$  in  $\text{CDCl}_3$

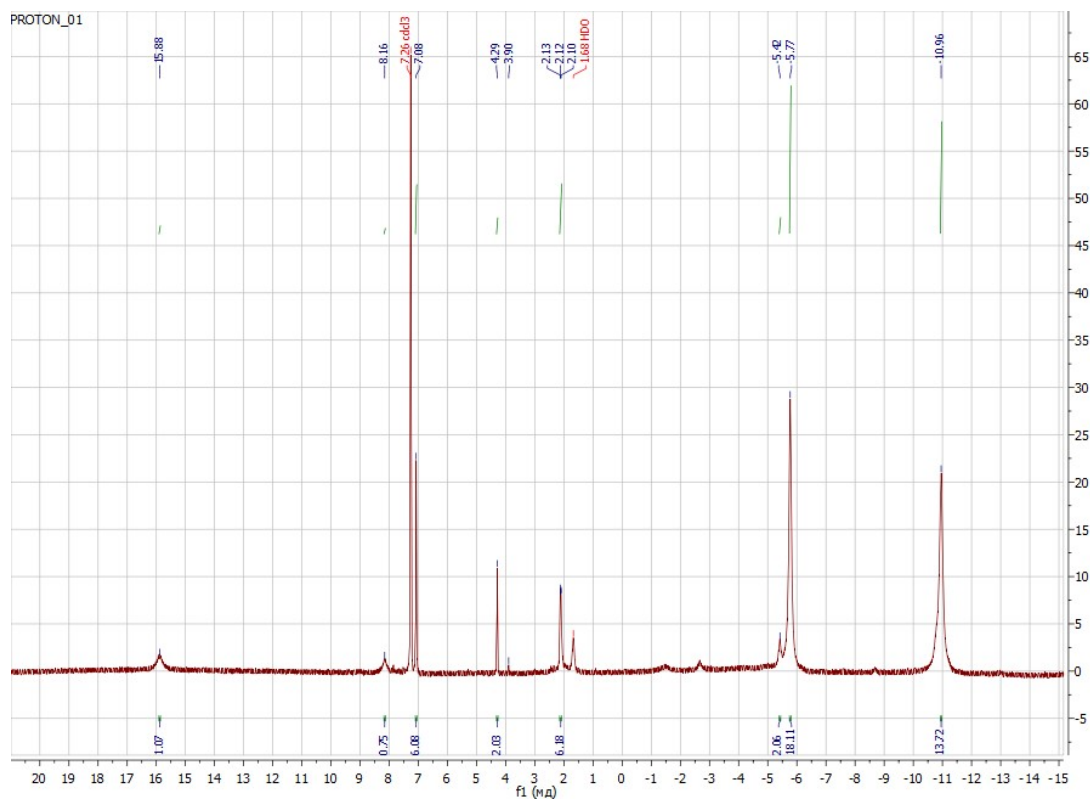
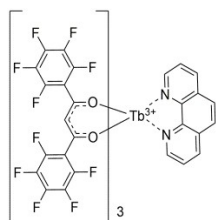


Figure S119.  $^1\text{H}$ - NMR spectrum of  $[\text{Tb}(\text{PFDMB})_3\text{Phen}]$  in  $\text{CDCl}_3$

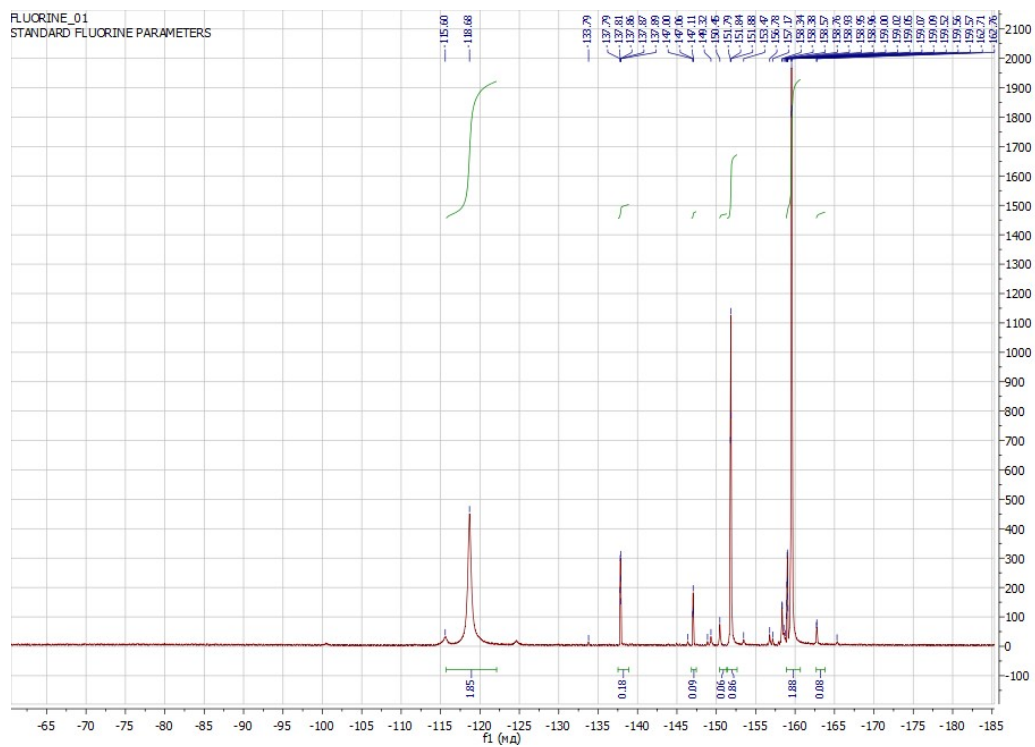


Figure S120.  $^{19}\text{F}$ - NMR spectrum of  $[\text{Tb}(\text{PFDMB})_3\text{Phen}]$  in  $\text{CDCl}_3$

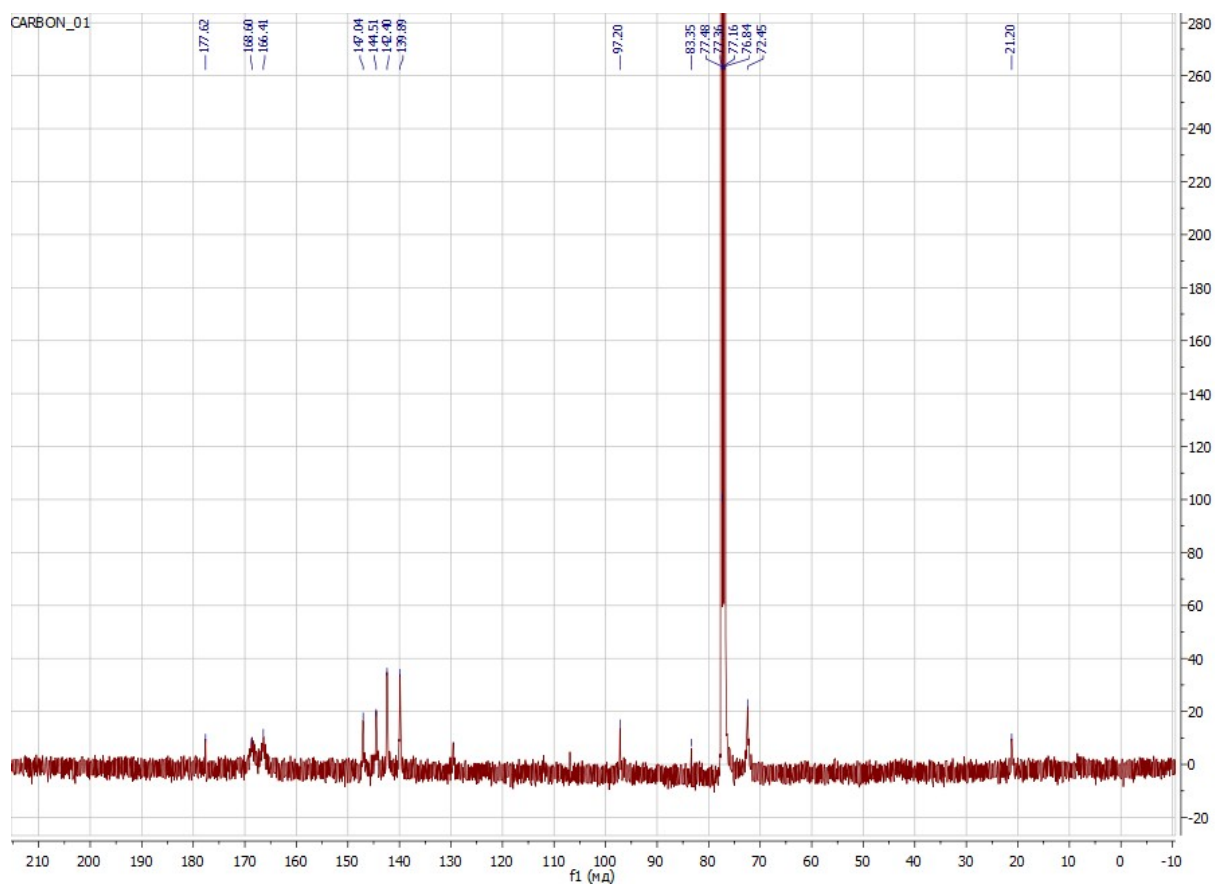


Figure S121.  $^{13}\text{C}$ - NMR spectrum of  $[\text{Tb}(\text{PFDMB})_3\text{Phen}]$  in  $\text{CDCl}_3$

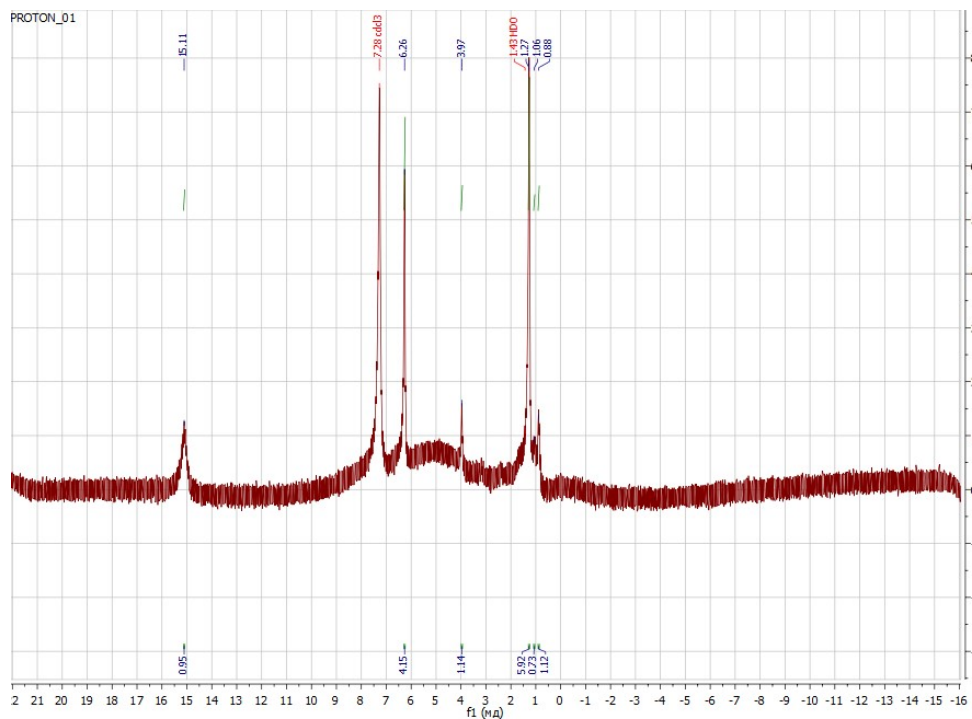
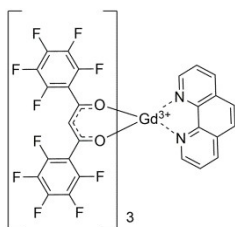


Figure SI22.  $^1\text{H}$ - NMR spectrum of  $[\text{Gd}(\text{PFDMB})_3\text{Phen}]$  in  $\text{CDCl}_3$

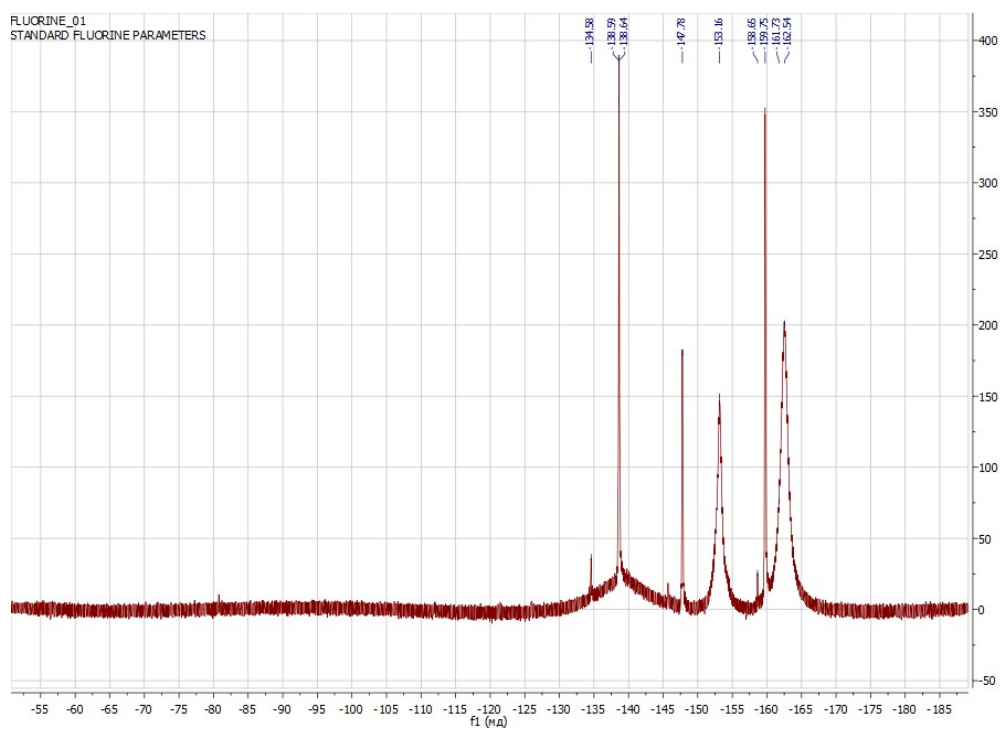
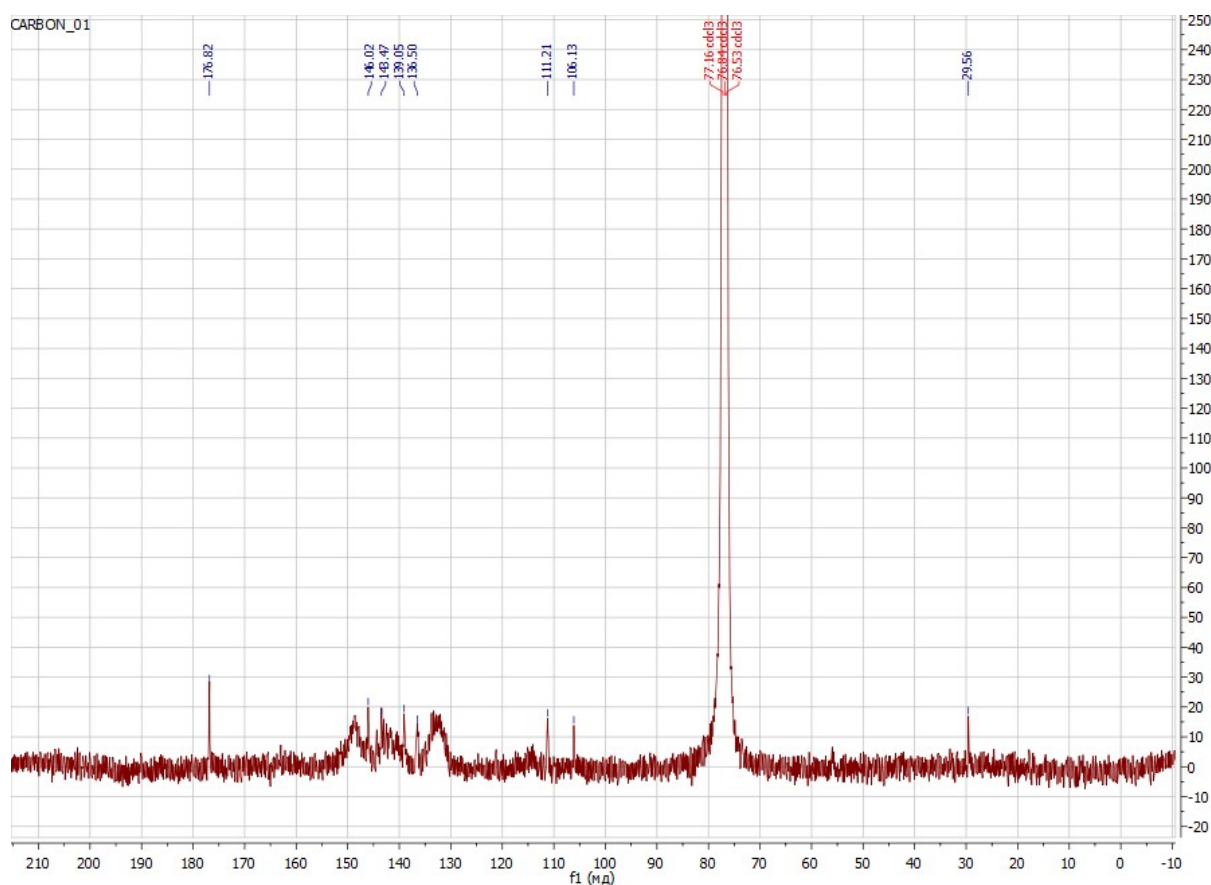


Figure SI23.  $^{19}\text{F}$ - NMR spectrum of  $[\text{Gd}(\text{PFDMB})_3\text{Phen}]$  in  $\text{CDCl}_3$



**Figure SI24.**  $^{13}\text{C}$ - NMR spectrum of  $[\text{Gd}(\text{PFDMB})_3\text{Phen}]$  in  $\text{CDCl}_3$

## References

1. Freidzon AYa, Scherbinin AV, Bagaturyants AA, Alfimov MV. Ab Initio Study of Phosphorescent Emitters Based on Rare-Earth Complexes with Organic Ligands for Organic Electroluminescent Devices. *J Phys Chem A*. 2011;115(18):4565-4573. doi:10.1021/jp111303a
2. Korshunov VM, Tsorieva AV, Gontcharenko VE, et al. Photophysical Properties of  $\text{Eu}^{3+}$   $\beta$ -Diketonates with Extended  $\pi$ -Conjugation in the Aromatic Moiety. *Inorganics*. 2022;11(1):15. doi:10.3390/inorganics11010015
3. Hasegawa Y, Kitagawa Y, Shoji S. Energy Transfer of Lanthanide Coordination Compounds. In: *Lanthanide-Based Wavelength Conversion Materials*. Springer Nature Singapore; 2024:71-118. doi:10.1007/978-981-97-5636-0\_4
4. Hori A, Shinohe A, Takatani S, Miyamoto TK. Synthesis and Crystal Structures of Fluorinated  $\beta$ -Diketonate Metal ( $\text{Al}^{3+}$ ,  $\text{Co}^{2+}$ ,  $\text{Ni}^{2+}$ , and  $\text{Cu}^{2+}$ ) Complexes. *Bulletin of the Chemical Society of Japan*. 2009;82(1):96-98. doi:10.1246/bcsj.82.96
5. Kusakawa T, Sakai S, Nakajima K, Yuge H, Rzeznicka II, Hori A. Synthesis, Structures and Co-Crystallizations of Perfluorophenyl Substituted  $\beta$ -Diketone and Triketone Compounds. *Crystals*. 2019;9(3):175. doi:10.3390/cryst9030175

